International Communications in Heat and Mass Transfer 37 (2010) 372–378

Contents lists available at ScienceDirect

International Communications in Heat and Mass Transfer

journal homepage: www.elsevier.com/locate/ichmt

Energy and exergy analyses in drying process of porous media using hot air ☆

Ratthasak Prommas, Phadungsak Rattanadecho *, Dulyachot Cholaseuk

Research Center of Microwave Utilization in Engineering (R.C.M.E.), Department of Mechanical Engineering, Faculty of Engineering, Thammasat University; (Rangsit Campus), Pathumthani 12120, Thailand

ARTICLE INFO

Available online 24 February 2010

Keywords:
Energy
Exergy
Drying porous medium
Capillary pressure

ABSTRACT

In this paper the energy and exergy analyses in drying process of porous media using hot air was investigated. Drying experiments were conducted to find the effects of particle size and thermodynamics conditions on energy and exergy profiles. An energy analyses was performed to estimate the energy utilization by applying the first law of thermodynamics. An exergy analyses was performed to determine the exergy inlet, exergy outlet, exergy losses and efficiency during the drying process by applying the second law of thermodynamics. The results show that energy utilization ratio (EUR) and exergy efficiency depend on the particle size as well as hydrodynamic properties. Furthermore, the results of energy and exergy presented here can be applied to other porous drying processes which concern effect of porosity as well as grain size.

1. Introduction

Drying is widely used to preserve porous medium products. It is a complicated process involving heat and mass transfer between the material surface and its surroundings [1]. Thermal drying in solids might be regarded as a result from two simultaneous actions: a heat transfer process by which the moisture content of the solid is reduced and a mass transfer process that implies fluid displacement within the structure of the solid towards its surface. Such motion depends on medium structure, moisture content and characteristics of the material. Furthermore the separation of vapor from solid substrate depends also on external pressure and temperature distribution on the total area of solid surface and the moisture content of drying air. Provided that thermal drying occurs in slow rate at ambient conditions, thus drying plants are designed and developed in order to accelerate appropriate drying rates for example, to supply the product is more heat those of ambient conditions [2]. Transferring in porous media is an important research subject that can be applied to various industrial applications, such as chemical reactors, heat exchangers, thermal insulations, electronic cooling and etc. Two distinguish approaches are taken into consideration to study transfer mechanisms in porous media [3]. One of the main goals in designing and optimizing of industrial drying processes is to use as little to reduce moisture from the product to the desired value. Consequently, energy quantity and quality as well as heat and mass transfer should be investigated throughout progressive drying process [4]. The concepts of exergy destruction, exergy consumption, irreversibility, and lost work are importance. Exergy is a measurement of the maximum useful work that can be done by a system interacting with an environment at a constant pressure and temperature. The simplest is that of a reservoir with heat source of infinite capacity and invariable temperature. The maximum efficiency of heat withdrawal from a reservoir that can be converted into work is called the Carnot efficiency [5].

The features of exergy are identified to highlight its importance in a wide range of applications [6]. Exergy analysis has been increasingly as a useful tool in the design, assessment, optimization and improvement of energy systems [7]. It can be applied on both system and component levels. Exergy analysis leads to a better understanding of the influence of thermodynamic phenomena on effective process, comparison of the importance of different thermodynamic factors, and the determination of the most effective ways of improving the process [8]. As regards the exergy analyses of drying processes, some work has been carried out in recent years. Dincer and et. al [9] analyzed a thermodynamic aspect of the fluidized bed drying process of large particles for optimizing the input and output conditions by using energy and exergy models. The effects of the hydrodynamic and thermodynamic conditions were also analyzed such as inlet air temperature, fluidization velocity and initial moisture content on energy efficiency and exergy efficiency. Dincer and Sahin [10] used a model to analyze exergy losses of air drying process. Their work demonstrated that the usefulness of exergy analysis in thermodynamic assessments of drying processes and providence the performances and efficiencies of these processes. Akpinar [11,12] studied energy and exergy of the drying of red pepper slices in a convective

☆ Communicated by W.J. Minkowycz.

* Corresponding author.
E-mail address: ratphadu@engr.tu.ac.th (P. Rattanadecho).

0735-1933/$ – see front matter © 2010 Elsevier Ltd. All rights reserved.
doi:10.1016/j.icheatmasstransfer.2009.12.006

Nomenclature

c_p	specific heat, (kJ/kg K)
C_p	mean specific heat, (kJ/kg K)
EUR	energy utilization ratio, (%)
Ex	exergy, (kJ/kg)
g	gravitational acceleration, m/s^2
g_c	constant in Newton's law
h	enthalpy, (kJ/kg)
J	joule constant
$\dot{m}$	mass flow rate, (kJ/s)
N	number of species
P	pressure, (kPa)
Q	net heat, (kJ/s)
Q_u	useful energy given by heater, (kJ/s)
s	specific entropy, (kJ/kg K)
T	temperature, (K)
U	specific internal energy, (kJ/kg)
v	specific volume, m^3/s
V	velocity, (m/s)
w	specific humidity, (g/g)
$\dot{W}$	energy utilization, (J/s)
z	altitude coordinate, (m)

Subscripts

a	air
da	drying air
d	drying chamber
f	fan
i	inlet
L	loss
mp	moisture of product
o	outlet
pb	porous packed bed
sat	saturated
∞	surrounding or ambient

Greek symbols

φ	relative humidity, (%)
η_{ex}	exergetic efficiency, (%)
μ	chemical potencial, (kJ/kg)

type dryer, with potato slices in a cyclone type dryer and pumpkin slices in a cyclone type dryer. The type and magnitude of exergy losses during drying was calculated. Colak and Hepbasli [13] performed an exergy analysis of thin layer drying of green olive in a tray dryer. In Colak's [14] study the effects of the drying air temperature, the mass flow rate of drying air and olives on the system performance were discussed. Ceylan et al. [15] carried out energy and exergy analyses during the drying of two types of timber. The effects of ambient relative humidity and temperature were taken into account.

The drying of porous media has been interested by many researchers and become complex, coupled, and multiphase processes with a wide range of applications in industry. In addition, as a result of high cost of energy, an operation with a high potential for optimizing with respect to energy savings has been realized. For many years, it has been studied experimentally for measuring drying kinetics on the macro-scale.

Typical applications of non-uniform material include the tertiary oil recovery process, geothermal analysis, asphalt concrete pavements process and preservation process of food stuffs. Therefore, knowledge of heat and mass transfer that occurs during convective drying of porous materials is necessary to provide a basis for fundamental understanding of convective drying of non-uniform materials.

The fore mentioned works concerned mainly with, energy and exergy analyses of drying process. Normally, most of materials in the drying process are porous materials. In the recent works the authors were mention about porous materials structure, with are concern with energy and exergy analyses of drying process.

The objectives of this work are to evaluate (i) the exergy losses of two operations porous packed bed, (ii) the distributions of the exergy losses and exergy input of the different drying operations and (iii) the influences of operating parameters on exergy losses. The knowledge gained will provide an understanding in porous media and the parameters which can help to reduce energy consumptions and losses.

2. Experimental apparatus

Fig. 1(a) shows the experimental convective drying system. The hot air, generated electrically travels through a duct toward the upper surfaces of two samples situated inside the test section. The outside walls of test section are covered with insulation to reduce heat loss to the ambient. The outlet flow and temperature can be adjusted at a control panel.

As shown in Fig. 1(b), the samples are unsaturated packed beds composed of glass beads, water and air. The samples are prepared in the two configurations: a single-layered packed bed (uniform packed bed) with bed depth 50 mm ($d = 0.15$ mm (F bed) and $d = 0.4$ mm (C bed)). The width and total length of all samples used in the experiments are 50 mm and 100 mm, respectively. The temperature distributions within the sample are measured using fiberoptic sensors (LUXTRON Fluroptic Thermometer, Model 790, accurate to 0.5), which are placed in the center of the sample at inserted into the packed bed at 5, 15 and 25 mm. form surface in Fig. 2. In each test run, the weight loss of the sample is measured using a high precision mass balance.

The uncertainty in the results might come from the variations in humidity and room temperature. The uncertainty in drying kinetics is assumed to result from errors in the measuring weight of the sample. The calculated uncertainties in weight in all tests are less than 2.8%. The uncertainly in temperature is assumed to result from errors in adjusting input power, ambient temperature and ambient humidity. The calculated uncertainty associated with temperature is less than 2.85%.

3. Mathematical formulation of problem

Schematic diagram of the convective drying model for porous packed bed is shown in Fig. 3. When a packed bed is heated by hot air flowing over its upper surface, the heat is transferred from the top of packed bed into the interior. Therefore, the temperature gradient is formed in the bed, and the liquid phase at the upper surface of packed bed evaporates by the variation of saturated vapor concentration corresponding to this temperature gradient as long as the surface remains wetted. In analysis, the main assumptions involved in the formulation of the transport model are:

1. The capillary porous material is rigid and no chemical reactions occur in the sample.
2. Local thermodynamic equilibrium is reached among each phase.
3. The gas phase is ideal in the thermodynamic sense.
4. The process can be modeled as steady-flow.
5. Packed bed sample side wall is perfectly insulated, hence adiabatic.

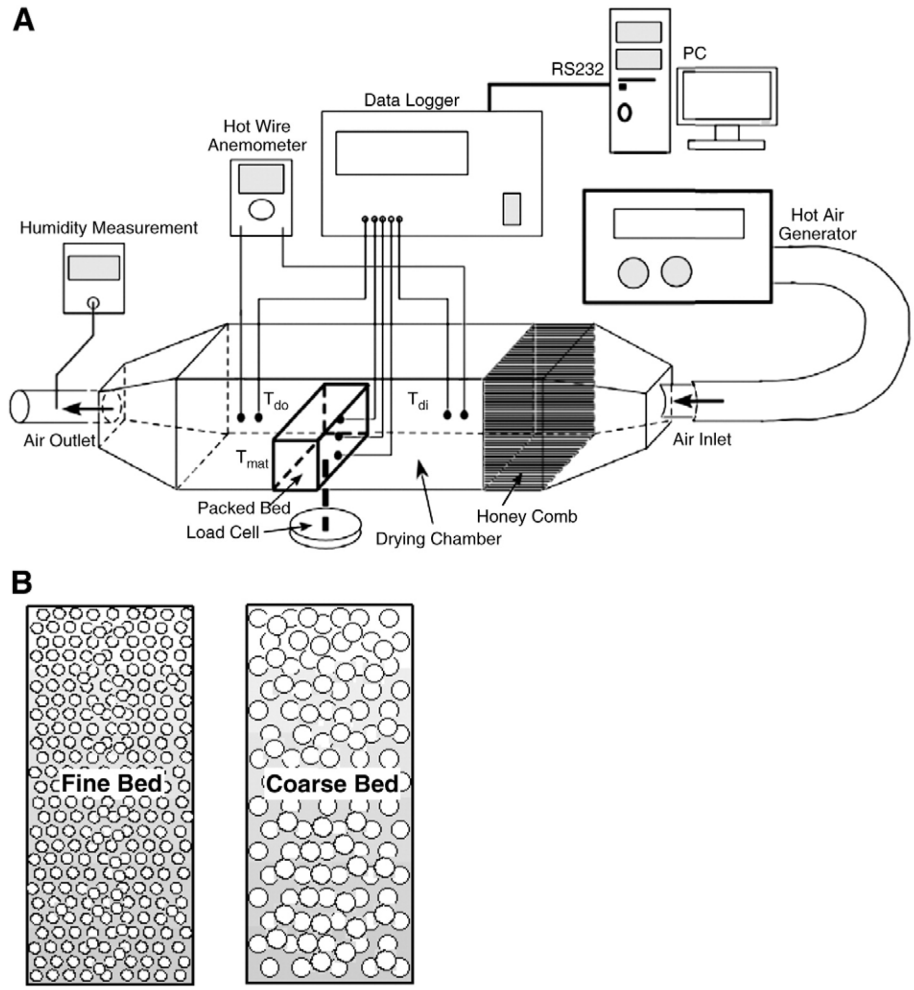

Fig. 1. Schematic of experimental facility: (a) Equipment setup; (b) Porous packed beds of different particle sizes (sample).

6. In a macroscopic sense, the packed bed is assumed to be homogeneous and isotropic, and liquid water is not bound to the solid matrix.
7. A dry layer (evaporation front) is formed immediately after water saturation approaches the irreducible value.

By energy and exergy analyses in drying process of single-layered packed bed using hot air, the main basic equations are given as follows:

3.1. Energy analysis

The traditional methods of thermal system analysis are based on the first law of thermodynamics. These methods use an energy balance on the system to determine heat transfer between the system and its environment. The first law of thermodynamics introduces the concept of energy conservation, which states that energy entering a thermal system with fuel, electricity, flowing streams of matter, and so on is conserved and cannot be destroyed. In general, energy balances provide no Information on the quality or grades of energy crossing the thermal system boundary and no information about internal losses (Fig. 4).

The drying process includes the process of heating, cooling and humidification. The process can be modeled as steady-flow processes by applying the steady-flow conservation of mass (for both dry air and

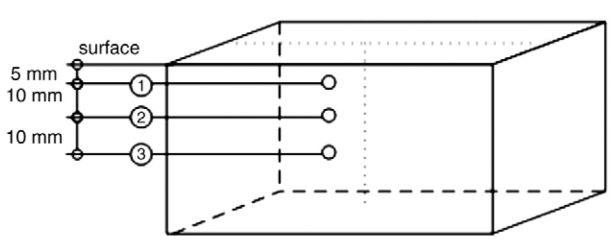

Fig. 2. The positions of temperature measurement in porous packed bed.

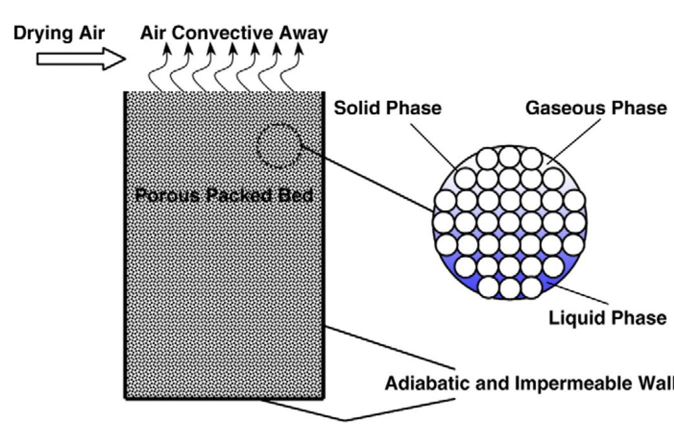

Fig. 3. Configuration of porous packed bed.

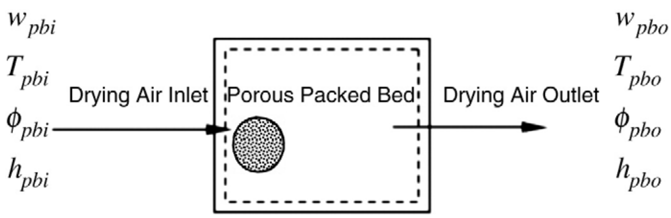

Fig. 4. Properties of porous packed bed in drying chamber.

moisture) and conservation of energy principles. General equation of mass conservation of drying air:

$$\sum \dot{m}_{ai} = \sum \dot{m}_{ao} \tag{1}$$

General equation of mass conservation of moisture:

$$\sum \left(\dot{m}_{wi} + \dot{m}_{mp}\right) = \sum \dot{m}_{wo} \tag{2}$$

or

$$\sum \left(\dot{m}_{ai} w_i + \dot{m}_{mp}\right) = \sum \dot{m}_{ai} w_o$$

General equation of energy conservation:

$$\dot{Q} - \dot{W} = \sum \dot{m}_o \left(h_o + \frac{V_0^2}{2}\right) - \sum \dot{m}_i \left(h_i + \frac{V_i^2}{2}\right) \tag{3}$$

where the changes in kinetic energy of the fan were taken into consideration while the potential and kinetic energy in other parts of the process were neglected. During the energy and exergy analyses of packed bed drying process, the following equations were used to compute the enthalpy of drying air.

$$h = c_{pda} T + w h_{sat@T} \tag{4}$$

The enthalpy equation of the fan outlet was obtained Bejan [16] using Eq. (5) as below:

$$h_{fo} = \left[\left(\dot{W}_f - \frac{V_{fo}^2}{2*1000}\right)\left(\frac{1}{\dot{m}_{da}}\right)\right] + h_{f_i} \tag{5}$$

where, h_{f_i} characterizes the enthalpy of drying air at the inlet of the fan, h_{fo} the enthalpy at the outlet of the fan, V_{fo} the drying air velocity at the outlet of the fan, W_f fan energy and $\dot{m}_{da}$ mass flow of drying air. Considering the values of dry bulb temperature and enthalpy from Eq. (5), the specific and relative humidity of drying air at the outlet of the fan were determined Akpinar [11]. The inlet conditions of the heater were assumed to be equal to the outlet conditions of the fan. The useful energy gained from the heater enters the drying chamber as the convection heat source, which was defined as:

$$\dot{Q}_u = \dot{m}_{da} c_{pda} (T_{ho} - T_{hi}) \tag{6}$$

where T_{ho}, T_{hi} are the outlet and inlet temperature of air at the heating section. The inlet conditions of the drying chamber were determined depending on the inlet temperatures and specific humidity of drying air. It was considered that the mass flow rate of drying air was equally passed throughout the chamber. The specific humidity at the outlet of the chamber can be defined as:

$$w_{pbo} = w_{pbi} + \frac{\dot{m}_{wpb}}{\dot{m}_{da}} \tag{7}$$

where $\dot{w}_{dci}$ denotes the specific humidity at the inlet of the chamber, $\dot{m}_{wpb}$ the mass flow rate of the moisture removed from packed bed samples. The heat utilized during the humidification process at the chamber, can be estimated by

$$\dot{Q}_{pb} = \dot{m}_{da}\left(h_{pbi@T} - h_{pbo@T}\right) \tag{8}$$

$$h = c_{pda} T + w h_{sat@T} \tag{9}$$

where w_{pbo} is the amount of product moisture evaporated. The energy utilization ratio for the drying chamber can be obtained using the following expression Akpinar [11]:

$$EUR_{dc} = \frac{\dot{m}_{da}(h_{dci@T} - h_{dco@T})}{\dot{m}_{da} c_{pds} (T_{ho} - T_{hi})} \tag{10}$$

4. Exergy analysis

The second law of thermodynamics introduces the useful concept of exergy in the analysis of thermal systems. As known, exergy analysis evaluates the available energy at different points in a system. Exergy is a measurement of the quality or grade of energy and it can be destroyed in the thermal system. The second law states that part of the exergy entering a thermal system with fuel, electricity, flowing streams of matter, or other sources is destroyed within the system due to irreversibilities. The second law of thermodynamics uses an exergy balance for the analysis and the design of thermal systems. In the scope of the second law analysis of thermodynamics, total exergy of inflow, outflow and losses of the drying chamber were estimated. The basic procedure for exergy analysis of the chamber is to determine the exergy values at steady-state points and the reason of exergy variation for the process. The exergy values are calculated by using the characteristics of the working medium from a first law energy balance. For this purpose, the mathematical formulations used to carry out the exergy balance are as show below Ahern [17].

$$Exergy = \underbrace{(u - u_\infty)}_{\text{internal energy}} - \underbrace{T_\infty (s - s_\infty)}_{\text{entropy}} + \underbrace{\frac{P_\infty}{J}(v - v_\infty)}_{\text{work}} + \underbrace{\frac{V^2}{2gJ}}_{\text{momentum}} + \underbrace{(z - z_\infty)\frac{g}{g_c J}}_{\text{gravity}}$$
$$+ \underbrace{\sum_c (\mu_c - \mu_\infty) N_c}_{\text{chemical}} + \underbrace{E_i A_i F_i \left(3T^4 - T_\infty^4 - 4T_\infty T^3\right)}_{\text{radiation emission}} + \ldots\ldots\ldots\ldots \tag{11}$$

The subscript ∞ denotes the reference conditions. In the exergy analyses of many systems, only some of the terms shown in Eq. (11) are used but not all. Since exergy is energy available from any source, it can be developed using electrical current flow, magnetic fields, and diffusion flow of materials. One common simplification is to substitute enthalpy for the internal energy and *PV* terms that are applicable for steady-flow systems. Eq. (11) is often used under conditions where the gravitational and momentum terms are neglected. In addition to these, the pressure changes in the system are also neglected because of $v \cong v_\infty$, hence Eq. (11) is reduced as

$$Exergy = \bar{c}_p \left[(T - T_\infty) - T_\infty \ln \frac{T}{T_\infty}\right] \tag{12}$$

The inflow and outflow of exergy can be found using the above expression depending on the inlet and outlet temperatures of the drying chamber. Hence, the exergy loss is determined as:Exergy

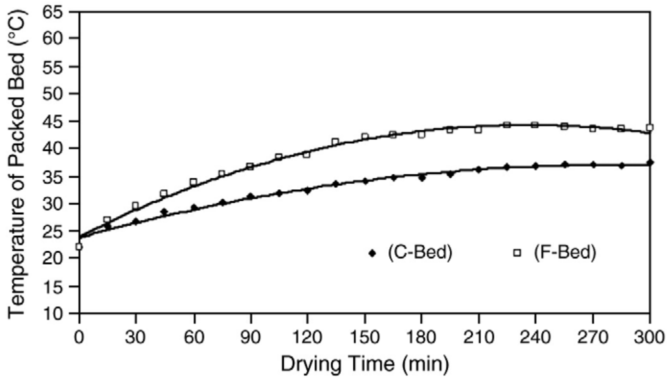

Fig. 5. The temperature profiles with respect to time.

loss = Exergy inflow − Exergy outflow

$$\sum Ex_L = \sum Ex_i - \sum Ex_o \tag{13}$$

The exergy inflow for the chamber is stated as below

$$Ex_{\rm dci} = Ex_{\rm pbi} = \bar{c}_{\rm p_{da}}\left[(T_{\rm dci} - T_\infty) - T_\infty \ln\frac{T_{\rm dci}}{T_\infty}\right] \tag{14}$$

The exergy outflow for the drying chamber is stated as:

$$Ex_{\rm dco} = Ex_{\rm pbo} = \bar{c}_{\rm pda}\left[(T_{\rm dco} - T_\infty) - T_\infty \ln\frac{T_{\rm dco}}{T_\infty}\right] \tag{15}$$

The exergetic efficiency can be defined as the ratio of the product exergy to exergy inflow for the chamber as outlined below:

$$Exergy\,Efficiency = \frac{Exergy\ inf\ low - Exergyloss}{Exergy\ inf\ low} \tag{16}$$

$$\eta_{Ex} = 1 - \frac{Ex_L}{Ex_i} \tag{17}$$

5. Results and discussions

Drying experiments were conducted by varying operating parameters which are temperature, air velocity, packed beds thickness and air humidity. For porous packed beds of two different sizes, 0.15 and 0.45 mm. drying air temperatures 50 °C and air velocities 2.5 m/s, energy and exergy analyses were carried out.

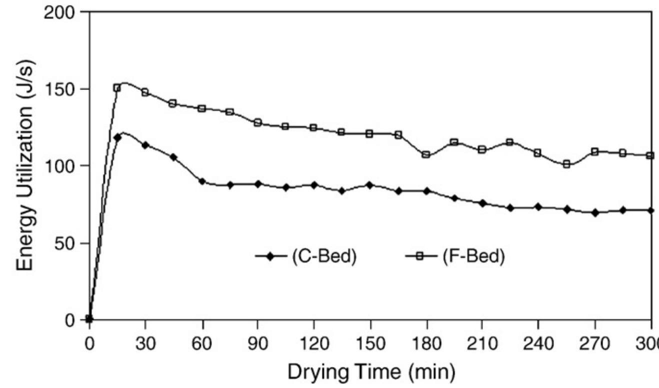

Fig. 7. Variation of energy utilization and drying time with different packed bed.

It is observed that at the early stage of the drying process the temperature profiles in both cases are nearly the same. As drying progresses, the temperature increases. This is because the latent heat transfer due to evaporation is retained due to the decline of the mass transfer rate together with the decreasing of average moisture content. Nevertheless, the temperature profile in F bed rises at a higher rate than that in the C bed. This is because the dry layer formed earlier in the F bed and an abrupt temperature rise occurs as the dry bulb temperature is approached. On the other hand, in the case of the C bed the temperature increases more slowly in comparison to F bed due to the late formation of dry layer. The prediction of the formation of a dry layer estimated from the drop in the surface mass of drying and rise in the drying temperature is marked in Fig. 5.

In the single-layered packed bed, the moisture content continuously decreases toward the surface. The decrease in surface saturation, this set up a saturation gradient, which draws liquid water toward the surface through capillary action while water vapor moves towards the surface due to a gradient in the vapor partial pressure. However, the internal moisture transport is mainly attributable to capillary flow of liquid water through the voids during the initial stage of drying.

Fig. 6. show the variation of moisture content and drying time. It is observed that at the early stage of the drying process the moisture content profiles in both cases are nearly the same. As drying progresses, the moisture content decreases. The following discussion is concerned with the effect of particle size on moisture migration mechanism under the same conditions for the single-layered packed bed. In Fig. 6, the observed moisture content profiles at the leading edge of the sample in the case of fine bed (F bed) are higher than those in the case of coarse bed (C bed). This is because of the fine bed or small particle size (corresponding to a higher capillary pressure) can cause moisture to reach the surface at a higher rate than in the case of

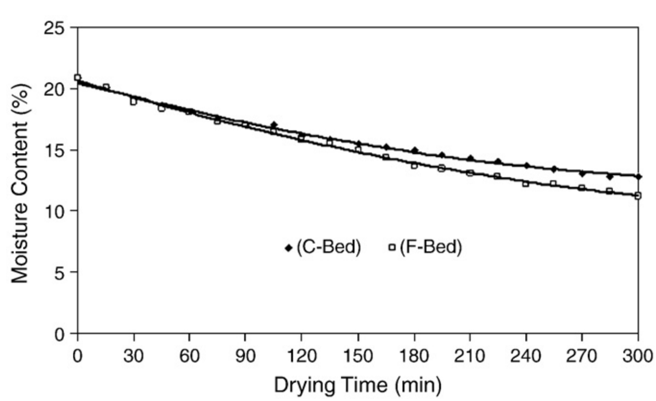

Fig. 6. The variation of moisture content with respect to time.

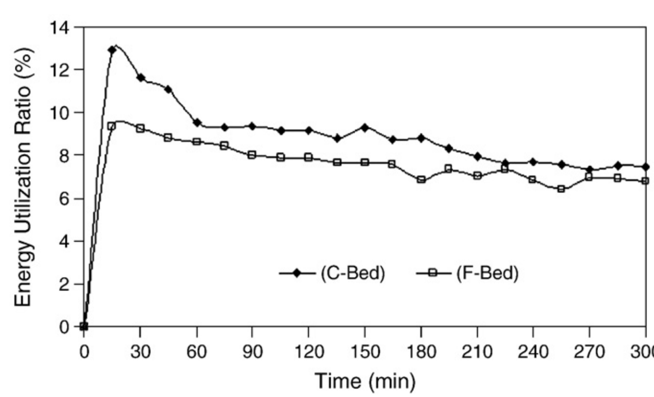

Fig. 8. Variation of energy utilization ratio with different packed bed.

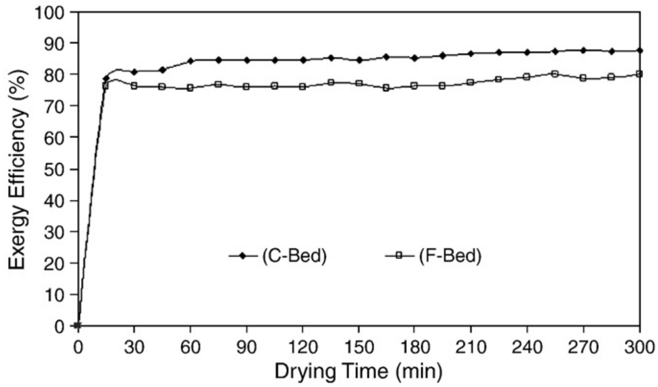

Fig. 9. Variation of exergy efficiency with different packed bed.

the coarse bed, i.e., large particle size. On the other hand, in the case of coarse bed, the moisture profiles at the leading edge of the sample are always lower as compared with the small particle size due to the lower capillary pressure inside the sample and the gravitational effect. Continued drying eventually causes the average moisture level inside the packed bed to decrease, especially at the leading edge of the upper layer (Fig. 6). When the moisture content at the upper surface (surface saturation) approaches the irreducible where the liquid water becomes discontinuous (pendular state), the liquid water supply to the surface by capillary action becomes insufficient to replace the liquid being evaporated. The latter arises from the fact that the dry layer takes place over small effective surface or on a front retreating from the surface into the interior of the sample dividing it into two layers, a dry layer and a two-phase layer. The discontinuity of the temperature gradient close to the drying front is a result of heat flux necessary for evaporation Pakdee and Rattanadecho [18]. In addition the effective thermal conductivity falls considerably resulting in a resistance of the heat flow rate. A further consequence of premature drying of the outer dry layer is that the local temperature of the sample will reach that of drying medium (hot air).

Fig. 7. shows the variation of energy utilization as a function of drying time for different particle sizes of particle and drying time. The energy utilization was high and getting higher at the beginning of drying process due to the high moisture of the sample while it quickly decreased because of the low moisture content of the samples towards the end of the process.

Fig. 8. shows the variation of energy utilization ratio (EUR) as a function of drying time for F bed and C bed. Energy balance analysis was carried to estimate the Energy Utilization Ratio (EUR). The values of the energy utilization in the drying chamber were calculated using Eq. (10). From the results it is observed that for a given particular air velocity during packed beds drying the EUR increases as particle size of packed bed decreases. These variations were more at the beginning of the drying and gradually the difference reduced Ratanadecho, Aoki and Akahori [19], this is because the large raise in particle size of packed bed significantly influences drying rate, hence at elevated particle size the EUR decreases with drying time. Consequently it was noticed that the EUR of drying chamber decreases with increase of drying time, it is because during the drying process the moisture content of the product decreases for the same energy input. Furthermore, at the beginning of the drying process, the energy efficiencies were observed to be higher than at the final stage and were found to be very low at the end of drying process.

Exergy analysis was carried to find the exergetic efficiency of the drying process Lampinen [20] by varying the drying parameters. The exergy inflow rates were calculated using Eq. (15) depending on the ambient and inlet temperatures. The exergy inflow during the drying of packed bed depending on drying particle size of packed bed. The exergy outflows were calculated using Eq. (16) and during the experiments which varied. It was observed that the exergy outflow from the drying chamber increased slowly with the drying time.

From the results it was noticed that the exergy outflow and the exergy loss increased with the increase of particle size. The exergetic efficiency of the drying chamber increased with the increase of drying time as shown in Fig. 9. This is because during the drying process the available energy in the drying chamber increases with drying time, since the amount of moisture decreases with time. Then, the effect of the other particle size on the drying time as well as the exergy efficiency of the drying system is presented. Furthermore, the exergy efficiencies of C-bed were observed to be higher than the F-bed about 10 % after 60 min of drying time with parallel to the end of drying process.

6. Conclusion

Energy and exergy analysis of the drying process of the packed bed were carried out in this study. Taking in to considerations the result from these analyses, the following conclusion may be drawn on energy utilization, energy utilization ratio and exergy efficiency decreased with increasing drying time, both energy utilization and energy utilization ratio increased with large particle size of packed bed.

The effects of particle sizes on the overall drying kinetics are clarified. The drying rate in the case of the F bed (fine particles) is slightly higher than that case of the C bed (coarse particles). This is because the higher capillary pressure for the F bed results in the maintenance of a wetted drying surface for a longer period of time.

It is also found that the drying rate depends strongly on the moisture content at the heating surface.

Our future aim is to validate the investigation of drying process of multi-layered packed beds. The comparisons of drying source between hot air and microwave energy.

Acknowledgments

The authors would like to express their appreciation to the Thailand Research Fund (TRF) for providing financial support for this study.

References

[1] K. Dutta, V.K. Nema, R.K. Bhardwaj, Drying behavior of spherical grains, Int. J. Heat Mass Transf. 31 (1988) 855–861.
[2] I. Dincer, A.Z. Sahin, A new model for thermodynamic analysis of a drying process, Int. J. Heat Mass Transf. 47 (2004) 645–652.
[3] B. Lyes, B. Azeddine, Mathematical description of heat and mass transfer during deep bed drying: effect of product shrinkage on bed porosity, Appl. Therm. Eng. 28 (2008) 2236–2244.
[4] E.K. Akpinar, A. Midilli, Y. Bicer, The first and second law analyses of thermodynamic of pumpkin drying process, J. Food Eng. 72 (2006) 320–331.
[5] M.A. Rosen, M.N. Le, I. Dincer, Efficiency analysis of a cogeneration and district energy system, Apply Therm. Eng. 25 (2005) 147–159.
[6] Yongzhong Liu, Yanfei Zhao, Xiao Feng, Exergy analysis for a freeze-drying process, Appl. Therm. Eng. 28 (2008) 675–690.
[7] M. Kanoglua, I. Dincer, M.A. Rosen, Understanding energy and exergy efficiencies for improved energy management in power plants, Energy Policy 35 (2007) 3967–3978.
[8] J. Szargut, D.R. Morris, F.R. Steward, Exergy Analysis of Thermal, Chemical and Metallurgical Processes, Hemisphere Publishing Corporation, New York, 1998.
[9] S. Syahrul, I. Dincer, F. Hamdullahpur, Thermodynamic modeling of fluidized bed drying of moist particles, Int. J. Therm. Sci. 42 (2003) 691–701.
[10] I. Dincer, A.Z. Sahin, A new model for thermodynamic analysis of a drying process, Int. J. Heat Mass Transf. 47 (2004) 645–652.
[11] E.K. Akpinar, Energy and exergy ananlyses of drying of red pepper slices in a convective type dryer, Int. Commun. Heat Mass Transf. 31 (8) (2004) 1165–1176.
[12] E.K. Akpinar, A. Midilli, Y. Bicer, Energy and exergy of potato drying process via cyclone type dryer, J. Food Eng. 46 (2005) 2530–2552.
[13] E.K. Akpinar, A. Midilli, Y. Bicer, The first and second law analyses of thermodynamic of pumpkin drying process, J. Food Eng. 72 (2006) 320–331.
[14] N. Colak, A. Hepbasli, Performance analysis of drying of green olive in a tray dryer, J. Food Eng. 80 (2007) 1188–1193.

[15] I. Ceylan, M. Aktas, H. Dogan, Energy and exergy analysis of timber dryer assisted heat pump, Appl. Therm. Eng. 27 (2007) 216–222.
[16] A. Bejan, Advanced Engineering Thermodynamics, John Wiley and Sons, New York, 1998.
[17] J.E. Ahern, The Exergy method of Energy Systems Analysis, John Wiley, New York, 1980.
[18] W. Pakdee, P. Rattanadecho, Unsteady effects on natural convective heat transfer through porous media in cavity due to top surface partial convection, Appl. Therm. Eng. 26 (2006) 2316–2326.
[19] P. Ratanadecho, K. Aoki, M. Akahori, Experimental and numerical study of microwave drying in unsaturated porous material, Int. Commun. Heat Mass Transf. 28 (2001) 605–616.
[20] M.J. Lampinen, M.A. Heikkinen, Exergy analysis for stationary flow systems with several heat exchange temperatures, Int. J. Energy Res. 19 (1995) 407–418.